Ultrastructure of Cultured Adult Myocardial Cells During Anoxia and Reoxygenation

P. SCHWARTZ, PhD, H. M. PIPER, MD, PhD, R. SPAHR, MA, and P. G. SPIECKERMANN, MD

From the Zentrum Anatomie and Zentrum Physiologie und Pathophysiologie, Universität Göttingen, Göttingen, FRG

Cultured heart cells from adult rats were exposed to anoxia in a substrate-free Tyrode's solution at constant pH. In this system the metabolic and the morphologic pattern can be investigated simultaneously. Anoxic changes develop gradually above 2 μmol adenosine triphosphate (ATP)/g_{ww}. Morphometry reveals that the morphologic changes are closely related to the energetic state: creatine phosphate (CP) decay is accompanied by the loss of small mitochondrial matrix granules (r = 0.97). The fall of ATP is coincident with sarcomere shortening (r = 0.95) and, below 4 μmol/g_{ww}, with mitochondrial swelling (r = −0.88). The number of lipid droplets correlates with the ATP level during anoxia and reoxygenation (r = −0.92). The early energetic depletion is accompanied by a moderate release of cytosolic enzymes and morphologic changes: the appearance of sarcolemmal microblebs and an increase in subsarcolemmal vesicles. Below an average ATP level of 2 μmol/g_{ww} an increasing number of individual cells fail to recover when reoxygenated. However, that failure is accompanied neither by massive enzyme release nor by ultrastructural damage regarded as typical for the "oxygen paradox." (Am J Pathol 1984, 115:349–361)

MORPHOLOGIC alterations in the hypoxic heart muscle can be related to biochemical changes only with difficulty.

1) From *in vivo* spectroscopy it is known that myocardial oxygen deficiency is not homogeneous throughout the heart.[1,2] Inhomogeneity may result from variations in vascular supply conditions, from variations in the cellular microenvironment, and from variations in the individual cellular response.

2) Usually, biochemical data represent average values for tissue specimens that also contain several nonmyocytic cell types.

3) Even with perfusion fixation, the preserved picture is not simultaneous with the biochemical results from a freeze-clamped specimen. Additionally, nonhomogeneity of intramural tension, which may be even further aggravated by the fixation process, may lead to varying degrees of artificial specimen damage during the processing for electron microscopy.[3]

Tissue slices *in vitro* have been used in attempting to overcome some of these difficulties.[4–6] Since Powell[7] had demonstrated that cardiocytes isolated from adult hearts could be exposed to physiologic media, an anoxia model of isolated heart cells seemed to be desirable. However, until recently only cell material with 20–40% of severely damaged cells could be obtained. Now, a procedure for purifying the isolated cell material to nearly 100% intact cells by culturing has been described.[8] We have used such short-term cultured ventriculocytes from adult rats for studying morphologic changes and their biochemical correlates during the early stage of oxygen deficiency.

Methods and Materials

Preparation and Anoxic Incubation of Cardiocytes

Ventricular muscle cells were isolated from 12-week-old female Sprague–Dawley rats and plated on dishes (60 mm Falcon dishes, Becton Dickinson, Oxnard, Calif) in M-199 medium containing 4% fetal calf serum, as previously described.[8]

After 4 hours' incubation, the dishes were washed and filled with 1 ml of a modified Tyrode's solution (125.0 mM NaCl, 2.6 mM KCl, 1.2 mM KH_2PO_4, 1.2

Supported by the Deutsche Forschungsgemeinschaft, SFB 89, Kardiologie Göttingen.

Accepted for publication January 5, 1984.

Address reprint requests to Dr. H. M. Piper, Zentrum Physiologie und Pathophysiologie, Abt. Herzstoffwechsel, Universität Göttingen, Humboldtallee 7, D-3400 Göttingen, FRG.

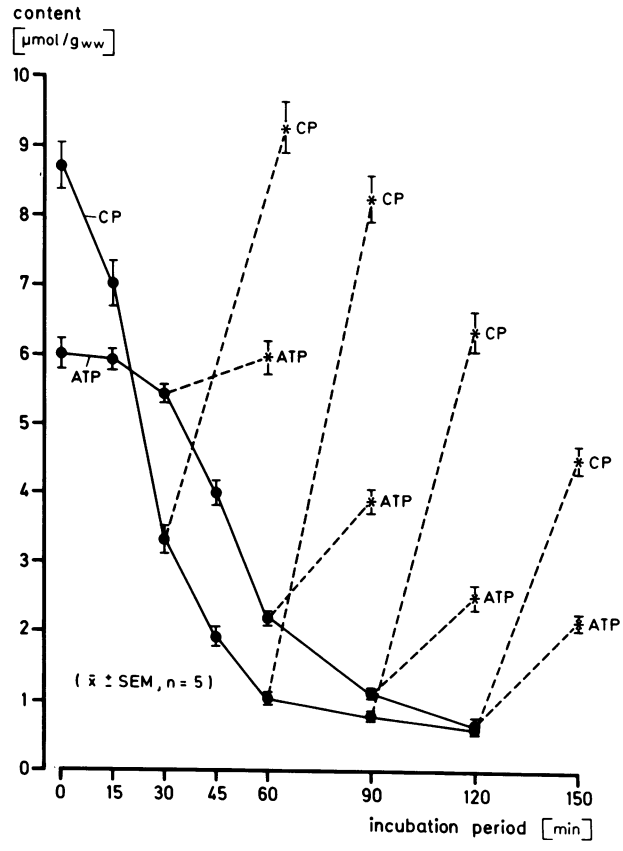

Figure 1 – Contents of ATP and CP during anoxia (*solid lines*) and reoxygenation (*broken lines, with asterisks*). All data are given as mean values ± SEM of 5 experiments performed under each specified incubation condition. (Kruskal-Wallis test: reoxygenated after 60 minutes of anoxia versus control, $P < 0.001$ for ATP, NS for CP; reoxygenated after 90 versus after 60 minutes of anoxia, $P < 0.001$ for both ATP and CP).

mM $MgSO_4$, 1.0 mM $CaCl_2$, 25.0 mM HEPES, pH = 7.4, equilibrated with 100% N_2 at 37 C) under a stream of nitrogen. Dishes were then transferred to air-tight incubation chambers that were gently perfused with water-saturated nitrogen and slowly rotated (1 cycle/5 min) at a slight inclination. Reoxygenation was performed by inflating 100% O_2 into the incubation chambers. Both perchloric acid for determination of metabolites and fixative solution for electron-microscopic studies were injected directly into the dishes kept under nitrogen or oxygen. With the same precaution, supernatant fluid was withdrawn for enzyme analysis. Oxygen measurements after 5 minutes of anoxic incubation revealed less than 1 mm Hg of oxygen in the supernatant. In all experiments pH was found to be between 7.35 and 7.4 under aerobic conditions as well as after 120 minutes of anoxia.

Analytic Procedures

Creatine phosphate (CP), adenosine triphosphate (ATP), adenosine diphosphate (ADP), adenosine monophosphate (AMP), and glycogen (as glucose) were assayed by the use of enzymatic standard procedures.[9] Lactate dehydrogenase (LDH, EC 1.1.1.27), malate dehydrogenase (MDH, EC 1.1.1.37) and glutamate dehydrogenase (GLDH, EC 1.4.1.3) were determined according to Bergmeyer.[9] Total enzyme activity was measured in cells from control dishes homogenized by ultrasound in 1 ml Tyrode's solution with 1% Triton X-100.

Dishes were routinely assayed for DNA content[10]; and from the relation of DNA to protein in myocytes and of protein content to wet weight in intact hearts, all data were expressed as referring to wet weight units. Cell content per 60-mm dish was measured as 4.5 ± 0.6 mg wet weight of cell material (mean ± SD) corresponding to about 10^5 cells.

Electron Microscopy

For electron microscopy, cells were fixed in 2% glutaraldehyde in 0.1 M cacodylate buffer at pH 7.3. The fixative solution was injected directly into the culture dishes kept under nitrogen or oxygen. After 2 hours fixation at 4 C, the cells were washed in buffer and postfixed in cacodylate-buffered 2% osmium tetroxide. For transmission electron microscopy (TEM), specimens were embedded in Araldite after dehydration. Ultrathin sections, cut parallel to the bottom of the dish, were stained with 2% methanolic uranyl acetate and lead citrate and examined in a Zeiss EM 10 microscope (Zeiss, Oberkochen, Germany).

For scanning electron microscopy (SEM) cells were fixed in the same way as for TEM. After dehydration in graded ethanols using amylacetate as intermedium, samples were dried in a Polaron critical point dryer (Polaron, Watford, England). After mounting on stubs, specimens were coated with gold/palladium in a cool sputter coater (Polaron) and examined in a Novascan 30 (Zeiss). Observations were made in a secondary electron mode at 15 kv.

Morphometry

Since the cell culture material was cut parallel to the bottom of the dish, all cells were cut along their longitudinal axis in a well-defined manner. In each experiment 20 micrographs, taken at random selection, represented a given incubation time. From 18 × 24-cm photographic prints (×27,000), the average

values for the number of mitochondrial granules, the mitochondrial area, and the sarcomere distance (Z-Z) were determined. Granular density was corrected for fictitious decrease due to mitochondrial volume swelling. For this, the volume extension was calculated from the enlarged cross-sections on the approximative assumption of a spherical shape of swollen mitochondria. Osmiophilic lipid droplets were counted from electron micrographs of whole longitudinal sections of randomly selected cells. Again, for a given incubation time, from 20 prints an average number was determined.

Variation coefficients of these averaged morphometric values were below 15% for three experiments independently performed under each specified condition.

Light-Microscopic Cell Counting

The ratio of polygonal cells with clearly discernible cross-striations to rounded cells was determined with a phase-contrast microscope (Zeiss) at ×400 magnification. Under each experimental condition, more than 1200 cells were examined after fixation in 2% glutaraldehyde. In doubtful cases, the cell was rather regarded as damaged, so that we would not overestimate the portion of rod-shaped cells.

Results

Metabolic Alterations

Under aerobic control conditions, the cultured cells contain physiologic levels of high-energy phosphates (Figure 1). Under anoxia, high-energy phosphate contents fall and, concomitantly, activities of cytosolic enzymes (LDH, MDH) increase in the extracellular space, while mitochondria-specific (GLDH) enzyme activities do not (Figure 2). MDH, about half of which is cytosolic,[9] is released only half as much as the cytosolic marker LDH. However, because MDH has the fourfold homogenate activity, in absolute terms its leakage is two times that of LDH. The anoxic release of cytosolic enzyme is highly correlated with the actual ATP content and therefore slows down when ATP degradation decelerates. This deceleration is most pronounced near 2 μmol ATP/g_{ww} (60 minutes' anoxia) where glycogen mobilization also distinctly decelerates, although only half of the initial amount of glycogen has been consumed (control, 43 ± 3; at 60 minutes, 22 ± 2; at 120 minutes, 18 ± 2 μmol glucose/g_{ww}).

During anoxia, the sum of ADP and AMP does not rise above 2 μmol/g_{ww}. Thus, the pool of adenine nucleotides is diminished with the fall of ATP. After reoxygenation, restored ATP levels do not exceed the actual amount of adenine nucleotides immediately before. Contrastively, CP is restored to a higher degree under reoxygenation.

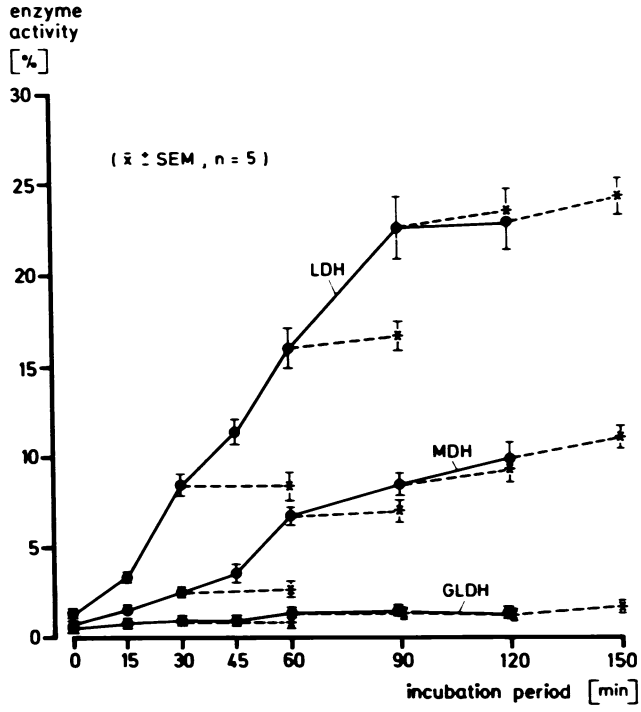

Figure 2—Enzyme release during anoxia (*solid lines*) and reoxygenation (*broken lines, with asterisks*). All data are given as mean values ± SEM of 5 experiments. At 15 minutes of anoxia, LDH and MDH activities differ significantly from control values ($P < 0.01$, Kruskal-Wallis test). Both anoxic LDH release and MDH release are correlated to the actual ATP content (for both, $r = -0.98$, $P < 0.001$). GLDH activity at 120 minutes of anoxia is not significantly different from the control value.

Morphometry

Initially the cell population contained 3.0 ± 1.6% round cells. Their number did not increase earlier than at 90 minutes of anoxia (60 minutes, 3.6 ± 1.5%, not significant versus control; 90 minutes, 14.1 ± 2.5%, $p < 0.001$ versus control; 120 minutes, 29.4 ± 4.7%; $P < 0.001$ versus 90 minutes; 120 minutes under aerobic control conditions, 3.7 ± 2.0%, not significant versus control; data are given as the mean ± SD, n = 5; statistical discrimination by the Kruskal-Wallis test). Up to 120 minutes of anoxia, reoxygenation does not change the number of round cells (n=5). Since even after 120 minutes of anoxia only a minor part of the population is irreversibly

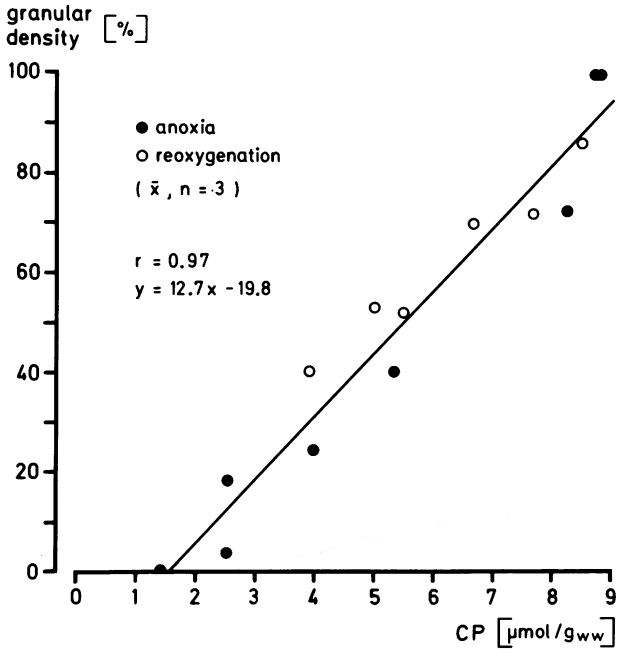

Figure 3—Relation of the average number of mitochondrial granules, expressed as a percentage of the control value, and CP content. Each point represents the mean value of 3 experiments.

overcontracted, morphometric average parameters related to biochemical changes show largely the same relations after reoxygenation as observed during the anoxic development (Figures 3–6).

Coincidently with CP decay, mitochondrial matrix granules vanish. At CP levels below one-third the initial value they disappear completely. Reoxygenation leads to reappearance of matrix granules in accordance with the extent of CP recovery (Figure 3).

In spite of the proceeding breakdown of energy-rich phosphates, mitochondria preserve their ultrastructure until ATP has fallen below 4 µmol ATP/g_{ww} (Figure 4). Below this level, mitochondrial swelling accompanies the loss of ATP. Again, reoxygenation reverses this development.

The numeric increase of lipid droplets coincides with the decrease of ATP levels. Readmission of oxygen decreases the droplet number again (Figure 5).

Loss of ATP is accompanied by a gradual decrease of sarcomere length. However, the maximal sarcomere length is observed at high ATP values, after the initial fall of CP. Therefore, sarcomere lengths at 6 µmol ATP/g_{ww} (Figure 6, in brackets) are shorter than slightly below that value. Using phase-contrast microscopy, we found a sarcomere length of 1.85 ± 0.08 µ (mean ± SD, n = 45) for unfixed, resting cells in aerobic Tyrode's solution.

Morphologic Details

Early Ultrastructural Changes (Figure 7)

Under aerobic control conditions, cultured cells exhibit a normal myocardial ultrastructure (A). Mitochondria contain many electron-dense matrix granules and have a dense cristal structure. There are abundant interfibrillar granules which are typical for glycogen deposits. The T-tubules are slightly distended.

At 15 minutes of anoxia, there are only minor changes when compared with the control picture (B). The number of matrix granules has decreased, and the T-system is widened.

At 30 minutes of anoxia, matrix granules have completely disappeared, but mitochondria are only slightly enlarged and have preserved their regular cristal structure (C). Glycogen granules are less, but still numerous. Z-Z distances are almost normal. In the proximity of mitochondria osmiophilic lipid droplets are seen. The nuclear chromatin becomes slightly marginated (D). As a first sign of structural alterations, large vesicles appear in the perinuclear area, which may correspond to enlarged lysosomes, endoplasmic reticulum, or mitochondrial residues.

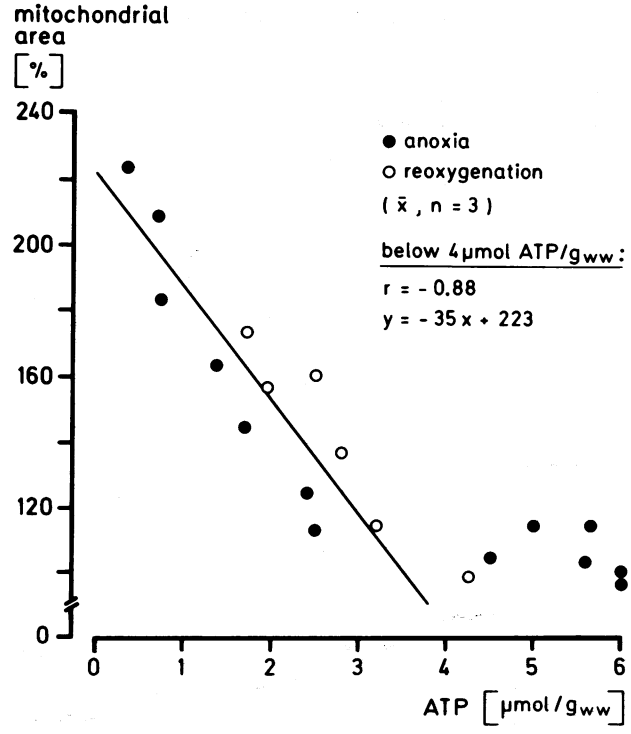

Figure 4—Relation of the average area of mitochondrial cross-sections, expressed as a percentage of the control value, and ATP content.

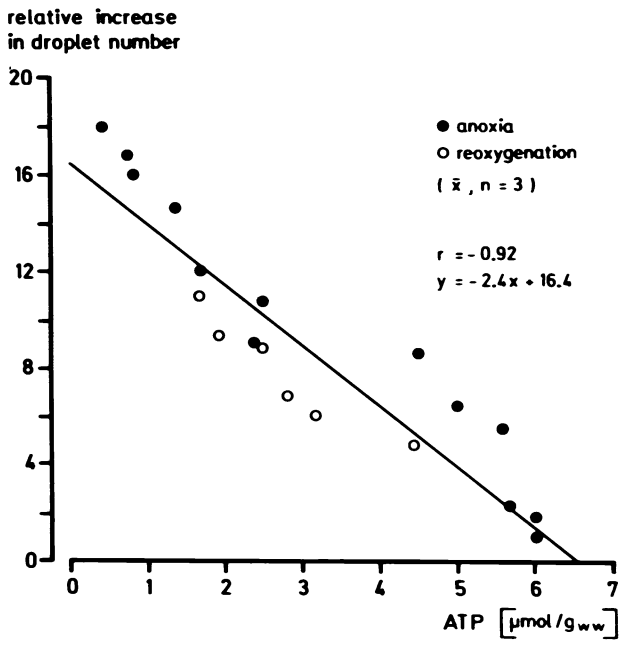

Figure 5 — Relation of the average number of lipid droplets, expressed as a multiple of the control value, and ATP content.

Early Sarcolemmal Alterations (Figure 8)

At 30 minutes of anoxia, it becomes apparent that the sarcolemma also undergoes structural changes: microblebs, not seen under control conditions (A), protrude from the cell surface, first at the intercalated disk areas (B), later in increasing number along the whole length of the cells. They develop a pearlike shape (C) and partly seem to become tied off from the surface. At 60 minutes of anoxia these microblebs are found spread over the surface of all polygonal cells. For this anoxic period they do not tend to be confluent. Typically, these microblebs contain single mitochondria (C).

Concomitantly with the appearance of microblebs the number of subsarcolemmal vesicles increases. Occasionally these vesicles are observed to communicate with the external space (D).

Recovery of Anoxic Cells (Figure 9)

At 60 minutes of anoxia, mitochondria are swollen. However, there seem to be two intermixed populations which differ considerably in the extent of swelling (A). Of two adjoining mitochondria, one exhibits an almost normal fine structure, while the other shows an extensive matrix clearing and distortion of its cristae. These translucent mitochondria are more numerous in the perinuclear space, thus emphasizing this as an area of particular sensitivity. Sarcomeres become definitely shortened now, with disappearance of discernible subsarcomeral bands. The T-system is narrower again. Glycogen is more reduced than before.

Up to 60 minutes of anoxia, 30 minutes of reoxygenation leads to full ultrastructural recovery (B). Only minor signs are reminiscent of the anoxic period: the T-system is enlarged, and glycogen granules are reduced. Again, the mitochondrial matrix reveals a regularly dense structure with embedded small matrix granules.

At 120 minutes of anoxia, the majority of mitochondria exhibit extensive matrix clearing now (C). However, there are still a few with dense cristae. The outer mitochondrial membranes are continuous and neither large intramitochondrial densities nor paracristal aggregations[11] are seen. Frequently, vesicles containing some amorphous material are seen near mitochondria. Sarcomeres are in contracture. In the whole cell the number of lipid droplets, mainly those near mitochondria, is markedly increased.

After prolonged anoxia an increasing number of

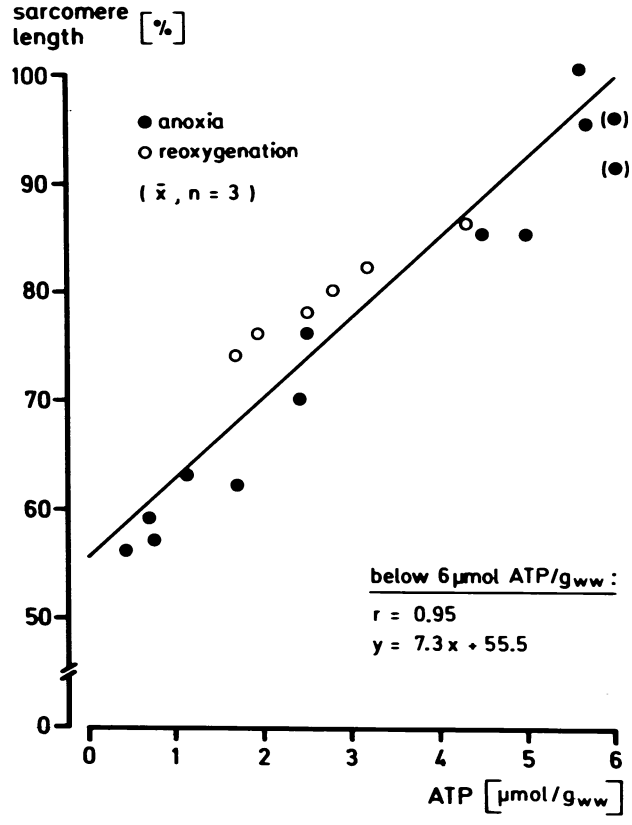

Figure 6 — Relation of the average Z-Z distance, expressed as a percentage of the maximal average distance observed, and ATP content. Distances at 6 µmol ATP/g_{ww} indicated by brackets (aerobic control at 91%).

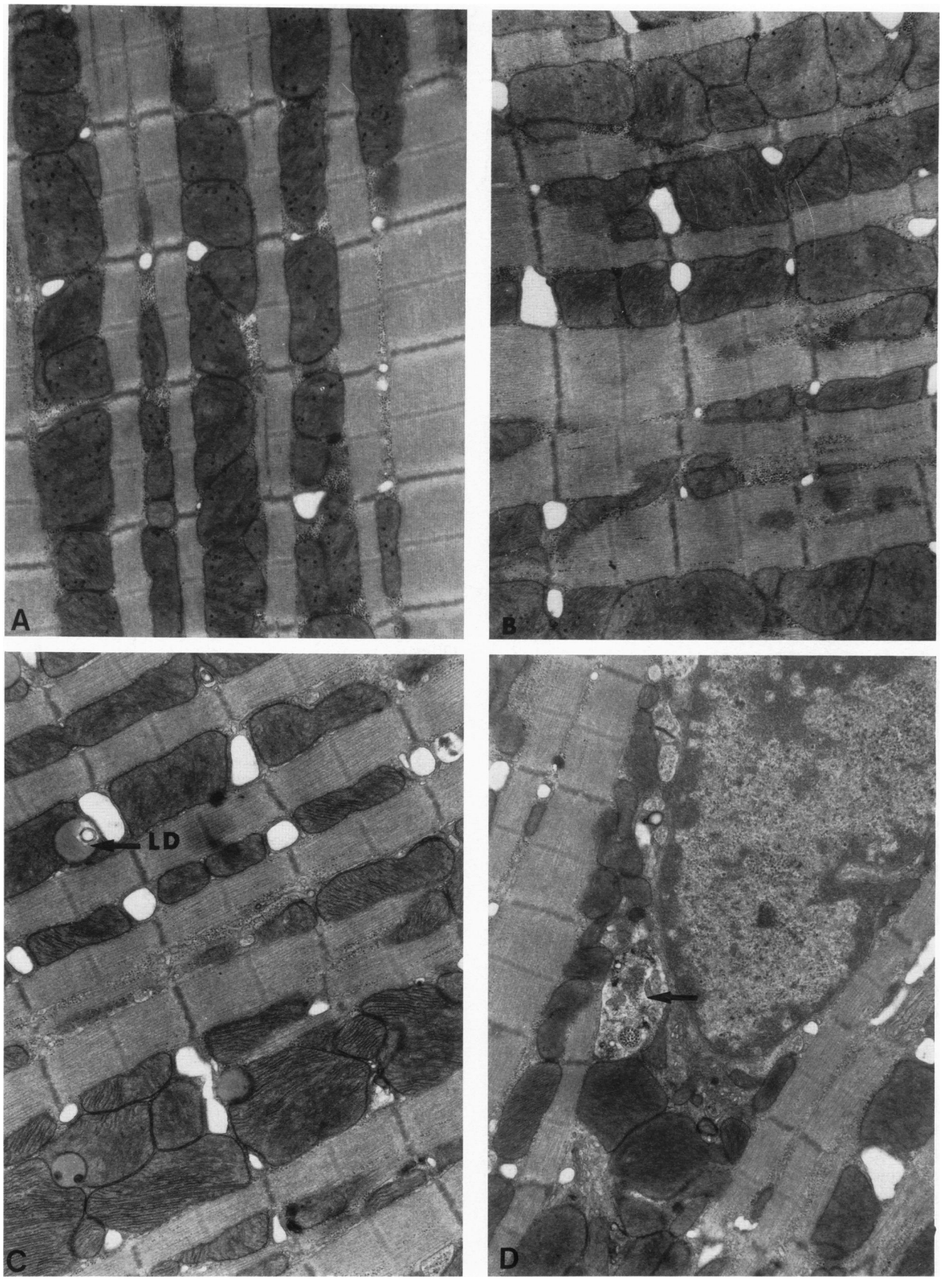

Figure 7 — Early ultrastructural changes. **A** — Aerobic control. Normal ultrastructure with relaxed myofibrils, electron-dense matrix granules, and abundant glycogen between myofibrils. (TEM, × 17,200) **B** — Fifteen minutes of anoxia. Reduction of electron-dense matrix granules. Widened T-system. (TEM, × 17,200) **C** — Thirty minutes of anoxia. Absence of electron-dense matrix granules, lipid droplets (*LD*, *arrow*). (TEM, × 17,200) **D** — Thirty minutes of anoxia. Perinuclear area. Nucleus with slightly marginated chromatin, vesicle containing amorphous material (*arrow*). (TEM, × 17,200)

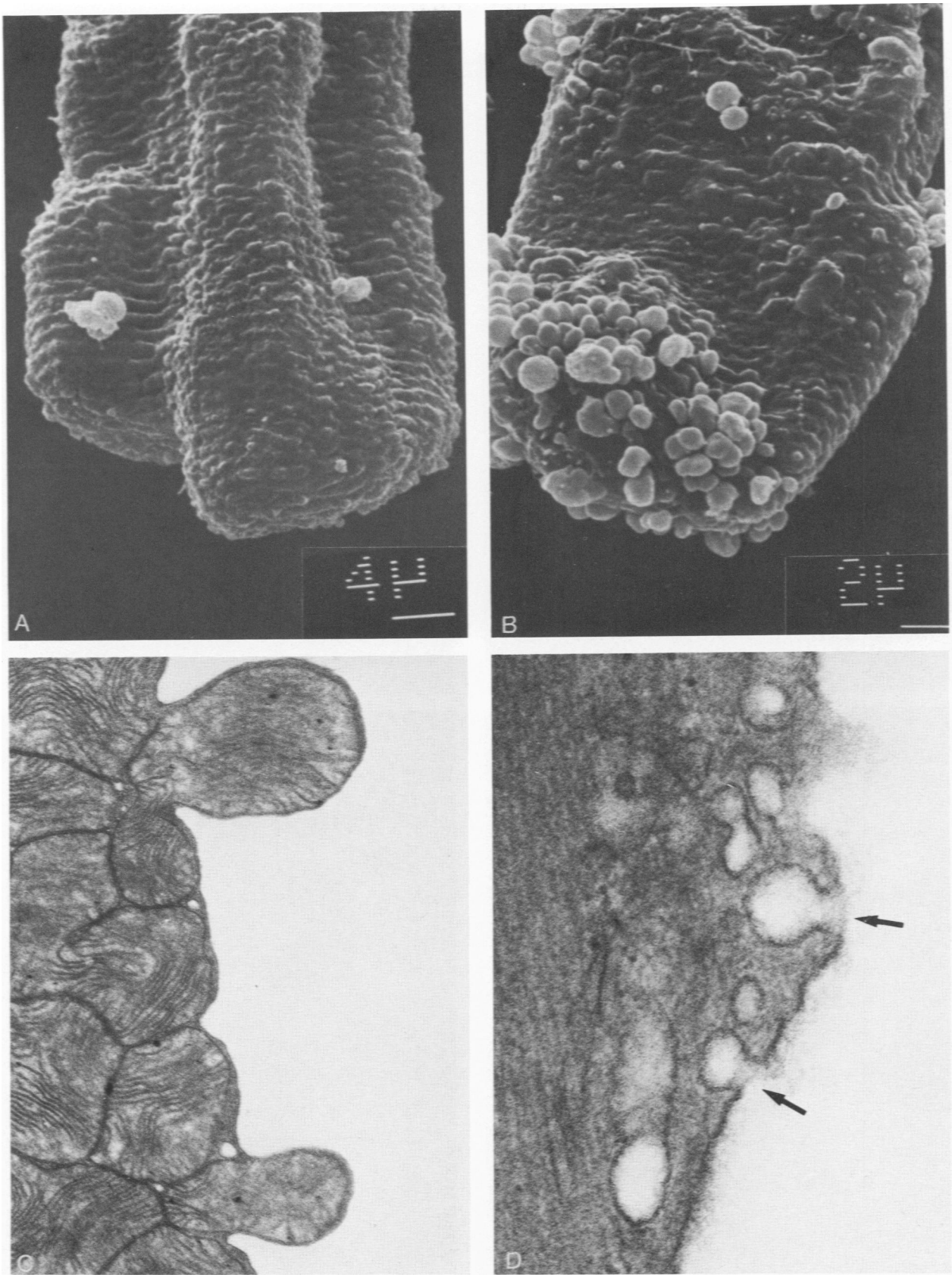

Figure 8 – Early sarcolemmal alterations. **A** – Aerobic control. View of the intercalated disk area. Smooth surface. (SEM) **B** – Thirty minutes of anoxia. Microblebs protruding from the cell surface near the intercalated disk area. (SEM) **C** – Thirty minutes of anoxia. Microblebs filled with a single mitochondrion. (TEM, × 28,200) **D** – Thirty minutes of anoxia. Subsarcolemmal space with numerous vesicular structures. partly communicating with the external space (*arrows*). (TEM, × 150,000) (With a photographic reduction of 3%)

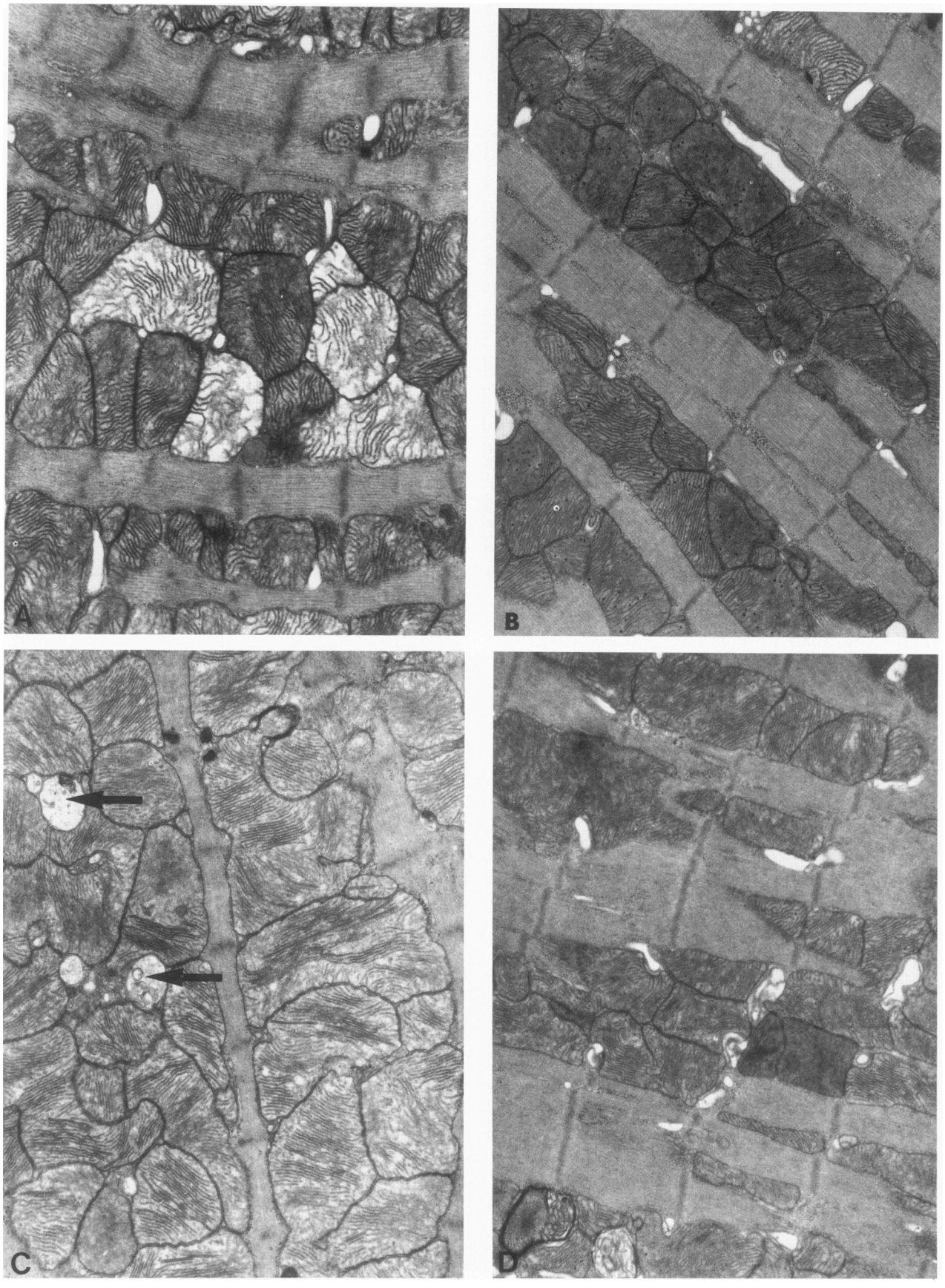
A
B
C
D

cells fail to recover. But at 120 minutes of anoxia, still the majority of cells recover when reoxygenated. After 30 minutes under oxygen, these recovering cells have almost regained a normal ultrastructure (D). However, mitochondrial matrix granules are fewer than in the control case, and the T-system is enlarged.

Anoxic Cell Deterioration (Figure 10)

At 90 and 120 minutes of anoxia, an increasing number of cells undergo apparently terminal alterations: they are overcontracted, and myofibrils are often condensed to homogeneous masses. Their surface is covered with large protrusions (A and B), mostly packed with mitochondria. These large protrusions differ in diameter considerably from the early developing microblebs (10–30 μ versus 1 μ). Mitochondria in these cells appear damaged to different degrees. While several exhibit an almost empty cristal space, many look even less damaged than those of polygonal cells after the same anoxic period. When reoxygenated, overcontracted cells retain these morphologic features. Neither contraction bands nor intramitochondrial densities develop. Sarcolemmal discontinuities are atypical. Polygonal cells recover when reoxygenated. At 120 minutes of anoxia their surface is covered with numerous microblebs (C). In reoxygenated populations, only minute remnants of these blebs are occasionally seen on polygonal cells (D).

Discussion

Comparison With Anoxic Tissue

In this cell culture system most cells have no structural connections. Thus, they are free of mechanical constraints as present in tissue. In addition, they are exposed to the same environmental conditions. Therefore, variations observed in the behavior of individual cells must be attributed to variations in their own properties.

The process of metabolic changes in anoxic cell cultures resembles that of the oxygen-deficient heart. However, the time course of changes is comparatively long, probably because these cultured cells are in diastolic rest. As known for the ischemic heart,[12,13] glycogen reserves do not limit cellular survival. In several studies it has been reported that an ATP content of 2 μmol/g_{ww} is a critical threshold below which recovery *ad integrum* is no longer possible.[13,14] Again, also in cell culture, this ATP level is critical. Below it, more and more cells become irreversibly overcontracted.

Ultrastructural alterations of the myocardial cell during oxygen deficiency and after reoxygenation have been investigated not only in the ischemic organ but also in anoxic perfused hearts[15] and tissue slices.[4,5] Apart from differences in the time course, the basic features of the ultrastructural development have been reported to be identical in all tissue systems in oxygen deficiency. Our isolated cell system has pH stability and low lactate accumulation in common both with the anoxic perfused heart and incubated thin tissue slices.

The Reversible Stage of Anoxia

The most prominent early sign of oxygen deficiency in myocardial cell culture is the gradual disappearance of the small mitochondrial matrix granules, closely related to the decrease of CP.[16] Apparently these granules consist mainly of organic material[17,18] that can be quickly mobilized when the cytosolic energy balance is changing.[19] Swelling of the T-system and occasionally the longitudinal parts of the sarcoplasmic reticulum are also concomitant with early energy disturbance.

With declining ATP levels sarcomeres shorten (Figure 6). It is not yet fully known why ATP depletion can induce contracture of the myocardial cell or the "stone heart" of the organ.[20,21] An important factor might be the disturbed ion balance of energy-depleted cells.[22] The development of cellular shortening may be found more pronounced in this isolated cell system than in whole hearts, because there are no external constraints that may antagonize contracture development in local ischemia.[23]

Under control conditions, a rather low sarcomere length (1.85 μ) is observed,[24,25] which is probably due to zero resting tension.[26] Then, during the stage of CP decay, a 10% larger sarcomere length is observed. This cannot be compared with sarcomere dilations in local ischemia, which are related to later stages of energy deficiency[23,27] and are possibly due to extension caused by the surrounding tissue.[23] Interestingly, that kind of dilation has not been observed in ischemic tissue slices.[5] Two explanations may be given for the initial extension in our system: either myofibrils relax with decay of CP, indicating an active com-

Figure 9 – Recovery of anoxic cells. **A** – Sixty minutes of anoxia. Nonhomogeneous mitochondrial swelling, marked sarcomere shortening. (TEM, × 17,200) **B** – Thirty minutes of reoxygenation after 60 minutes of anoxia. Reappearance of electron-dense matrix granules and relaxed myofibrils. (TEM, × 17,200) **C** – One hundred twenty minutes of anoxia. Homogeneous mitochondrial swelling. Large vesicles containing amorphous material (*arrows*). (TEM, × 17,200) **D** – Thirty minutes of reoxygenation after 120 minutes of anoxia. Recovering cell. Reduction of mitochondrial swelling and sarcomere shortening. (TEM, × 17,200)

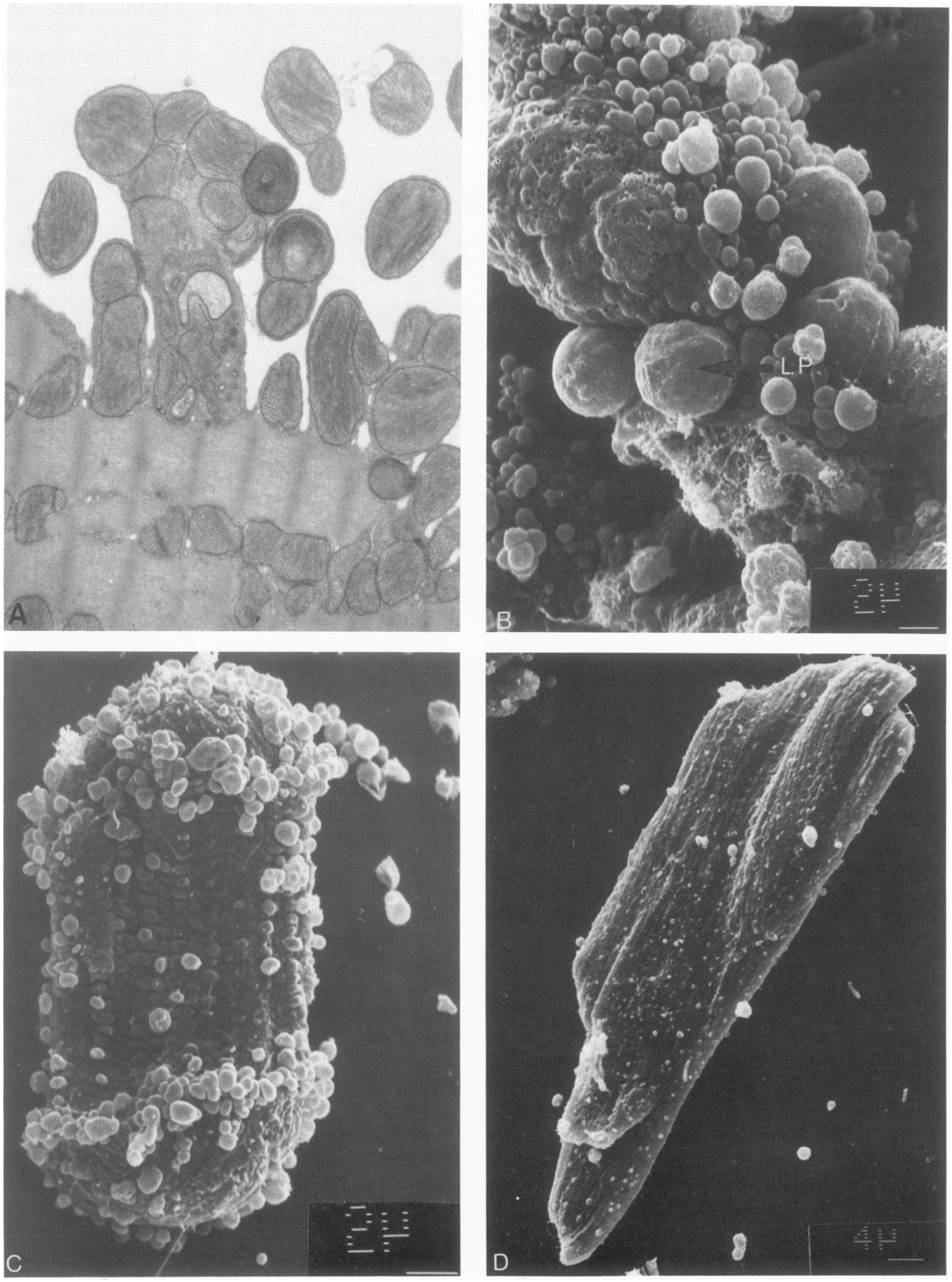

Figure 10 — Anoxic cell deterioration. **A** — One hundred twenty minutes of anoxia. Deteriorating cell. Protrusion of large sarcolemmal pouches filled with cell organelles. Overcontracted myofibrils. (TEM, × 17,200) **B** — One hundred twenty minutes of anoxia. Deteriorating cell. Cell surface consisting of protrusions of varying size. (SEM) **C** — One hundred twenty minutes of anoxia. Contracted cell of polygonal shape, covered with microblebs. (SEM) **D** — Thirty minutes of reoxygenation after 120 minutes of anoxia. Recovering cell, regaining elongated shape. Few microblebs left on surface. (SEM) (With a photographic reduction of 3%)

ponent of the control state, or the impinging fixative induces a small contraction as long as the cell has the energetic ability to contract.[28]

In this preparation, loss of ATP seems to be a gradual process involving most of the cells as long as ATP is above 2 μmol/g_{ww} (60 minutes of anoxia). This gradual decrease in ATP content is accompanied by a gradual release of a limited amount of cytosolic protein. Up to 60 minutes of anoxia, polygonal cells do not become overcontracted and show extensive ultrastructural and metabolic recovery when reoxygenated. At 60 minutes of anoxia, the population contains 4% round cells, but 16% of the cytosolic marker LDH is released, and the mitochondrial marker GLDH is not released. These results speak in favor of the hypothesis that early enzyme release is due to reversible sarcolemmal alterations.[29]

The reversible features of microbleb formation and increase in subsarcolemmal vesicles may be causally related to the protein release. It might be suggested that the extrusion of cytosolic enzymes is mediated by vesicular transport. Fusing these vesicles with the sarcolemma could enhance the sarcolemmal tension in a shortening cell, thus causing the propulsion of microblebs.

Mitochondrial swelling starts at 4 μmol ATP/g_{ww} (Figure 4). In contrast to the earlier gradual disappearance of small matrix densities, mitochondrial swelling develops nonhomogeneously throughout the mitochondrial population. The mitochondrial mass of an individual cell apparently consists of two subpopulations of differing sensitivity which are intermixed throughout the sarcoplasm. It is known from our studies[30] and the work of others[31-33] that heart mitochondria can be subdivided into two distinct classes by density centrifugation, both of which contain functionally intact mitochondria, which have, however, differing susceptibility to ischemic damage. It might be suggested that the morphologically different subpopulations observed in anoxic myocardial cells correspond to those separated *in vitro*. The morphologic difference is only a transient phenomenon. This may be the reason similar observations have seldom been reported for ischemic tissue,[34] in which the anoxic process is faster.

As shown in Figure 5, the accumulation of osmiophilic lipid droplets is strongly correlated to the actual ATP content. Compared with the observations of other authors,[19,35] this accumulation starts rather early. Since there is no external source in our cell culture system, these lipids have to come from internal sources.[35-37] It might be speculated that they contain mainly triacylglycerols.[38] Since the synthesis of this storage form of fatty acids requires ATP, the accumulation stops when ATP reserves are exhausted. If oxygen becomes available again, these stores are emptied, because fatty acids can be oxidized or used for membrane repair. One conclusion can be drawn for certain, namely, that lipid droplet formation is not a sign of irreversible injury. Indeed, deposition of endogeneously liberated lipids in neutral fat droplets may protect the cell from the deleterious biochemical and physical effects of these compounds.[39]

The Stage of Progressive Anoxic Damage

The presented data suggest that above an ATP level of 2 μmol/g_{ww}, metabolic and morphologic changes are gradual and similar throughout the population. However, the cells differ considerably in their ability to survive at low energy levels. Thus, a summation of "quantum steps"[40] leads to the death of the whole population. Later than 60 minutes of anoxia, ATP degradation and glycogen mobilization nearly stop, indicating a standstill of active metabolic processes. In polygonal cells, all mitochondria have a cleared matrix space with diffuse cristal membranes. I-bands disappear and Z-bands become thickened and often distorted. Sarcomeres are contracted to varying degrees; at 120 minutes of anoxia, on the average they have two-thirds the length observed initially. The T-system is squeezed.

At 120 minutes of anoxia, a third of all cells are round, containing overcontracted and distorted myofibrils. Myofibrils may be condensed to homogeneous masses but such a condensation is never confined to segments of the myofibrilar apparatus. Cellular organelles are protruded or expelled from these cellular remnants in large sarcolemmal pouches. It is noteworthy that in these cells many mitochondria look much less damaged than in polygonal cells. In this cell culture system the cells do not lyse immediately when irreversibly overcontracted: sarcolemmal discontinuities are atypical, and enzyme release distinctly precedes any increase in number of round cells. In fact, enzyme release already decelerates when single cells start to deteriorate.

Reversibility of Anoxic Injury

During progressive anoxia, glycogenolysis almost stops. Only half of the initial amount of glycogen is used. Therefore, enough substrate for oxidative recovery is left in the system if the metabolic machinery is not irreversibly damaged. If the cells are reoxygenated for 30 minutes before the ATP content has fallen below 2 μmol/g_{ww}, the ultrastructure of all cells regains the appearance of fresh myocardium—except for a persistent reduction of glycogen granules. With the extensive recovery of CP levels, electron-

dense matrix granules reappear. Most probably because of the loss of total adenine nucleotides,[41,42] ATP levels recover only up to two-thirds of their initial value after 60 minutes of anoxia.

Also later than 60 minutes of anoxia, reoxygenation always leads to an ultrastructural improvement of the polygonal cells while not influencing the overcontracted round cells in their gradual disintegration process. Local contraction bands confined to a few sarcomeres[43,44] are seen neither in prolonged anoxia (up to 120 minutes) nor after reoxygenation. In a piece of tissue, they may be caused by an inhomogeneous development of tension in partly recovering tissue,[43] or they may be produced by nonhomogeneous fixation conditions as an artifact.[3] Various types of large intramitochondrial densities have been described as characteristic for progressive ischemic damage and late reperfusion.[11,45] They were only rarely seen in our preparation at up to 120 minutes of anoxia and after reoxygenation. These densities have been regarded as typical signs of irreversible cellular damage.[27,45] Their absence in the cultured cells may be due to the fact that they occur only at stages later in the anoxic development than investigated in this study. But then their appearance does not necessarily mark the "point of no return" on the cellular level. Since such mitochondrial changes have also been described for anoxic perfused hearts,[15] in which acidification plays only a minor role, the fixed pH of our system cannot be regarded as responsible for this deviation.

It has been suggested by others that the aggravation of ischemic tissue damage by late reoxygenation ("oxygen paradox") is mostly due to mechanical tissue constraints.[43,44] Different from isolated cells, muscle cells in tissue are exposed to the forces of neighboring cells that resume active contractions or begin contracture. Additionally, the sarcolemma of a cell in tissue is not free to follow the shortening of an overcontracting myofibrilar apparatus. Contraction bands may result when the sarcomeral anchoring to the cell membrane is locally destroyed. Intramitochondrial calcium precipitates and a massive loss of cellular enzymes then may be secondary to sarcolemmal rhexis caused by overstretching a labilized structure.[43] Our results are in accord with this hypothesis, since they show that irreversible anoxic injury of cells free of external constraints does not immediately turn into the cellular disintegration pattern which is typical for the "oxygen paradox."

Conclusions

This study demonstrates that oxygen deficiency in cultured adult cardiocytes induces metabolic and morphologic changes similar to those in whole tissue. The major morphologic changes are closely related to the actual energetic state of the cells. Above an ATP level of 2 μmol/g_{ww}, metabolic and morphologic changes are gradual and similar throughout the population. During this early phase of anoxia there is a gradual release of cytosolic enzymes from reversibly injured myocardial cells correlating with the depletion of energy reserves. Formation of sarcolemmal microblebs and subsarcolemmal vesicles both may be causally related structural events.

At low average ATP levels, the population becomes progressively nonhomogeneous, and not all cells recover when reoxygenated. In cells failing to recover under reoxygenation, ultrastructural alterations regarded as characteristic for irreversible damage—eg, amorphous mitochondrial densities, sarcolemmal discontinuities, or contraction bands—are not typical. This supports the hypothesis that in tissue all these detrimental effects are consequences of mechanical cell-to-cell interactions. Therefore, it seems doubtful that the readmission of oxygen itself is deleterious, as suggested by the term "oxygen paradox."

References

1. Barlow CH, Chance B: Ischemic areas in perfused rat hearts: measurement by NADH fluorescence photography. Science 1976, 193:909–910
2. Steenbergen C, DeLeeuw G, Williamson JR: Heterogeneity of the hypoxic state in perfused rat heart. Circ Res 1977, 41:606–615
3. Bullock GR: Preservation of myocardium for ultrastructure and enzymatic studies, Enzymes in Cardiology: Diagnosis and Research. Edited by DJ Hearse, J de Leiris. New York, John Wiley & Sons, 1979, pp 461–479
4. Armiger LC, Gavin JB, Herdson PB: Mitochondrial changes in dog myocardium induced by neutral lactate in vitro. Lab Invest 1974, 31:29–33
5. Ganote CE, Jennings RB, Hill ML, Grochowski EC: Experimental myocardial ischemic injury: II. Effect of in vivo ischemia on dog heart slice function in vitro. J Mol Cell Cardiol 1976, 8:189–204
6. Jennings RB, Reimer KA, Hill ML, Mayer SE: Total ischemia in dog hearts, in vitro: 1. Comparison of high energy phosphate production, utilization, and depletion, and of adenine nucleotide catabolism in total ischemia in vitro vs. severe ischemia in vivo. Circ Res 1981, 49:892–900
7. Powell T, Twist VW: A rapid technique for the isolation and purification of adult cardiac muscle cells having respiratory control and a tolerance to calcium. Biochem Biophys Res Commun 1976, 72:327–333
8. Piper HM, Probst I, Schwartz P, Hütter FJ, Spieckermann PG: Culturing of calcium stable adult cardiac myocytes. J Mol Cell Cardiol 1982, 14:397–412
9. Bergmeyer HU: Methods of enzymatic analysis. New York, Academic Press, 1974
10. Oliver IT, Edwards AM, Pitot HC: Hormonal regulation of phosphoenolpyruvate carboxykinase in primary cultures of adult rat liver parenchymal cells. Eur J Biochem 1978, 87:221–227

11. Trump BJ, Mergner WJ, Kahng MW, Saladino AJ: Studies on the subcellular pathophysiology of ischemia. Circulation 1976, 53 (Suppl I): 17-26
12. Isselhard W: Das Verhalten des Energiestoffwechsels im Warmblüterherz bei künstlichem Herzstillstand. Pflügers Arch 1960, 271:347-360
13. Kübler W, Spieckermann PG: Regulation of glycosis in the ischemic and the anoxic myocardium. J Mol Cell Cardiol 1970, 1:351-377
14. Jennings RB, Hawkins HK, Lowe JE, Hill ML, Klotman S, Reimer KA: Relation between high energy phosphate and lethal injury in myocardial ischemia in the dog. Am J Pathol 1978, 92:187-214
15. Ganote CE, Seabra-Gomes R, Nayler WG, Jennings RB: Irreversible myocardial injury in anoxic perfused rat hearts. Am J Pathol 1975, 80:419-450
16. Paulussen F, Hübner G, Grebe D, Bretschneider HJ: Die Feinstruktur des Herzmuskels während einer Ischämie mit Senkung des Energiebedarfs durch spezielle Kardioplegie. Klin Wochenschr 1968, 46:165-171
17. Goldstein MA, Thyrum PT, Murphy DL, Martin JH, Schwartz A: Ultrastructural and contractile characteristics of isolated papillary muscle exposed to acute hypoxia. J Mol Cell Cardiol 1977, 9:285-295
18. Hagler H, Burton K, Buja L: Electron probe x-ray microanalysis of normal and injured myocardium: methods and results, Microprobe Analysis of Biological Systems. Edited by TE Hutchinson, AP Somlyo. New York, Academic Press, 1981, pp 127-155
19. Hatt PY, Moravec J: Acute hypoxia of the myocardium: Ultrastructural changes. Cardiology 1971/72, 56:73-84
20. Katz AM, Tada M: The "stone heart": A challenge to the biochemist. Am J Cardiol 1972, 29:578-580
21. Hearse DJ, Garlick PB, Humphrey SM: Ischemic contracture of the myocardium: mechanisms and prevention. Am J Cardiol 1977, 39:986-993
22. Hohl CM, Altschuld RA, Brierley GP: Effects of calcium on the permeability of isolated adult heart cells to sodium. Arch Biochem Biophys 1983, 221:197-205
23. Jennings RB, Ganote CE: Structural changes in myocardium during acute ischemia. Circ Res 1974, 35 (Suppl III): 156-172
24. Haworth RA, Hunter DR, Berkoff HA: Contracture in isolated adult rat heart cells: Role of Ca^{2+}, ATP, and compartmentation. Circ Res 1981, 49:1119-1128
25. Krueger JW, Forletti D, Wittenberg BA: Uniform sarcomere shortening behavior in isolated cardiac muscle cells. J Gen Physiol 1980, 76:587-607
26. Brady AJ: Mechanical properties of cardiac fibers, Handbook of Physiology, Sect 2, Vol I, The Heart. Edited by RM Berne, N Sperelakis, SR Geiger. Bethesda, Md, American Physiological Society, 1979, pp 461-496
27. Jennings RB, Sommers HM, Herdson PB, Kaltenbach JP: Ischemic injury of the myocardium. Ann NY Acad Sci 1969, 156:67-78
28. Caulfield J, Klionsky B: Myocardial ischemia and early infarction: An electron microscopic study. Am J Pathol, 1959, 35:489-523
29. Gebhard MM, Denkhaus H, Sakai K, Spieckermann PG: Energy metabolism and enzyme release. J Mol Med 1977, 2:271-283
30. Sezer O, Piper HM, Hütter JF, Spieckermann PG: Functional and structural alterations in defined subpopulations of ischemic cardiac mitochondria. Pflügers Arch 1982, 392 (suppl):R6
31. Whitty AJ, Dimino MJ, Elfont EA, Hughes GW, Repeck MW: Transmural mitochondrial differences in myocardium, Recent Advances in Studies on Cardiac Structure and Metabolism. Vol 11, Heart Function and Metabolism. Edited by T Kobayashi, T Sano, NS Dhalla. Baltimore, University Park Press, 1978, pp 349-354
32. Murphit RR, Stiles J, Powell WMJ, Sanadi DR: Experimental myocardial ischemia: Characteristics of isolated mitochondrial subpopulations. J Mol Cell Cardiol 1978, 10:109-123
33. Grieve SJ, Williams AJ: The isolation and characterization of cardiac mitochondrial fractions from isoprenaline treated rats. J Mol Cell Cardiol 1981, 13:705-714
34. Denker MW, Bergmann RA, Nachlas MM: Ultrastructural changes in myocardium during experimental ischemia. Johns Hopkins Med J, 1969, 124:311-329
35. Bilheimer DW, Buja LM, Parkey RW, Baute FJ, Willerson JT: Fatty acid accumulation and abnormal lipid deposition in peripheral and border zones of experimental myocardial infarcts. J Nucl Med 1978, 19: 276-283
36. Gordon GB, Barcza MA, Bush ME: Lipid accumulation in hypoxic tissue culture cells. Am J Pathol 1977, 88:663-678
37. Burton KP, Templeton GH, Hagler HK, Willerson JT, Buja LM: Effect of glucose availability on functional membrane integrity, ultrastructure and contractile performance following hypoxia and reoxygenation in isolated feline cardiac muscle. J Mol Cell Cardiol 1980, 12:109-133
38. Scheuer J, Brachfeld N: Myocardial uptake and fractional distribution of palmitate 1-^{14}C by the ischemic dog heart. Metabolism 1966, 15:945-954
39. Katz A, Messineo FC: Lipid-membrane interactions and the pathogenesis of ischemic damage in the myocardium. Circ Res 1981, 48:1-16
40. Ganote CE, Angelo J, Safavi S, Kaltenbach JP: Protection from irreversible hypoxic injury by potassium cardioplegia and hypothermia: Effects on contracture, morphology and O_2-enzyme release. J Mol Cell Cardiol 1982, 14:587-599
41. Kammermeier H: Verhalten von Adenin-Nucleotiden und Kreatinphosphat im Herzmuskel bei funktioneller Erholung nach länger dauernder Asphyxie. Verh Dtsch Ges Kreislaufforsch 1964, 30:206-211
42. Isselhard W, Mäurer W, Stremmel W, Krebs J, Schmitz H, Neuhof H, Esser A: Stoffwechsel des Kaninchenherzens in situ während Asphyxie und in der postasphyktischen Erholung. Pflügers Arch 1970, 316: 164-193
43. Ganote CE, Kaltenbach JP: Oxygen-induced enzyme release: Early events and a proposed mechanism. J Mol Cell Cardiol 1979, 11:389-406
44. Ganote CE: Contraction band necrosis and irreversible myocardial injury. J Mol Cell Cardiol 1983, 15:67-73
45. Jennings RB, Ganote CE: Mitochondrial structure and function in acute myocardial ischemic injury. Circ Res 1976, 38 (Suppl I):80-89

Acknowledgments

We greatly appreciate the technical assistance of R. Zöllner, M. Wucherpfennig, H. Haacke, and B. Eickhoff.